Histological and Bone Morphometric Evaluation of Osseointegration Aspects by Alkali Hydrothermally-Treated Implants

Hanako Umehara, Reiko Kobatake, Kazuya Doi *, Yoshifumi Oki, Yusuke Makihara, Takayasu Kubo and Kazuhiro Tsuga

Department of Advanced Prosthodontics, Hiroshima University Graduate School of Biomedical and Health Sciences, 1-2-3, Kasumi, Minami-ku, Hiroshima 734-8553, Japan; hanako-um@hiroshima-u.ac.jp (H.U.); reiko1122@hiroshima-u.ac.jp (R.K.); yos-oki14@hiroshima-u.ac.jp (Y.O.); yusuke0318@hiroshima-u.ac.jp (Y.M.); kubocky@hiroshima-u.ac.jp (T.K.); tsuga@hiroshima-u.ac.jp (K.T.)

* Correspondence: kazuya17@hiroshima-u.ac.jp; Tel.: +81-82-257-5677

Abstract: The purpose of this study was to investigate the osseointegration aspects of alkali-treated implants by histological and bone morphometric evaluations. Titanium implants (control) and alkali hydrothermally-treated titanium implants were used. Samples were evaluated by surface structure observation and wettability tests. Both implants were placed into the femurs of five rabbits, and osseointegration was assessed by measurement of removal torque (RT), bone–implant contact ratio (BIC), and bone tissue area ratio (BTA). Measurements were performed at the whole portion around the implant, the cortical bone portion, and the bone marrow portion. The surface structure of alkali-group showed nanoscale pores and super hydrophilicity. RT, BIC, and BTA values of alkali-group were significantly higher than those of control-group at the whole portion. In the cortical bone portion, the BIC value was higher in the alkali-group than in the control-group, and BTA showed no significant difference between groups. In the bone marrow portion, even though no significant difference between control and alkali groups, the latter had higher ratio of BIC than the former. These results indicate that alkali treated implants enhance bone integration in areas where the implant is in contact with bone, and may promote osteoinduction in the non-bone marrow portion.

Keywords: alkali hydrothermal treatment; osseointegration; dental implant

1. Introduction

Dental implants are widely used as prosthetic therapy for missing teeth. Implant therapy is considered to be successful when osseointegration is established and maintained over a long period of time [1–3]. Titanium has good biocompatibility and establishes both direct integration and osseointegration with the surrounding bone; thus, titanium is used as a dental implant material [4]. However, titanium is classified as a bioinert material, as it has no osteoinductive ability and does not chemically integrate with bone tissue.

The establishment and continuation of osseointegration are essential for supporting the implant; therefore, the development of an implant surface that achieves superior osteointegration has been essential in implant therapy.

Several studies have shown that titanium surface topography can be improved by various modification methods, including grit blasting, acid etching, alkali, strontium or magnesium hydrothermal treatment, and other methods [5–10]. Modification of the titanium surface enhances osteoblast activity and increases the area of contact between the implant and surrounding bone, thus facilitating osseointegration [5]. The improved osseointegration favors implant support. Many studies

have reported that a rough surface structure enhances bone integration and mechanical stability of implant [11], and promotes initial cell attachment and differentiation into osteoblasts [5,12]. In particular, titanium surfaces with a nanoscale surface structure enhance proliferation and differentiation of osteoblasts to a greater degree than mechanically polished surfaces and microscale surface structure [13–16].

The implant surface wettability impacts initial bone formation on the implant body. A super hydrophilic state indicates that the contact angle is extremely small (nearly 0 degrees); this state is advantageous to initial cell adhesion and can promote osseointegration.

Among several modification methods, alkali hydrothermal treatment is simple and non-invasive, and effectively creates a uniformly hydrophilic surface on the titanium surface. In addition, a titanium surface modified by a strong acid or alkali solution can form an apatite layer when it is soaked in simulated body fluid (SBF) [17–19].

In our previous study, a comparison between acid and alkali hydrothermal treatment of a titanium thin membrane was performed. Acid treatment produced macroscale rough structure on the titanium surface; however, mechanical strength was significantly decreased because of its corrosive action. In contrast, alkali hydrothermal treatment produced a nanoscale rough surface texture and a super hydrophilic structure, and the titanium was not strongly corroded during the process. Therefore, there was little influence on titanium structural change [20]. It has become clear that alkali hydrothermally-treated titanium implants promote osteogenesis and osseointegration, as determined by evaluation of the characteristics, a cell experiment, and an *in vivo* study [21]. Camargo et al. reported that alkali-based treated implants resulted in superior bone formation and bone integration between the bone and implant surface due to a nanoscale structure and titanate layer [22]. The alkali-treated surface topography was assumed to enhance the surface bioactivity on titanium implants and subsequently accelerate the early bone formation process. However, few studies have evaluated the histological and bone morphometric aspects of bone contact and bone formation in the bone–implant interface and surrounding bone. Thus, the detailed elements of bone formation of alkali hydrothermally-treated implants have not been clarified.

The purpose of the present study was to investigate the bone formation aspects of alkali hydrothermally-treated implants *in vivo* by histological and bone morphometric evaluations.

2. Materials and Methods

2.1. Sample Preparation

Pure titanium implants (implant body: diameter 2.0 mm, length 4 mm; implant head: diameter 3.0 mm; height 0.5 mm) (Nishimura Metal Co., Ltd., Fukui, Japan) were used in this study (Figure 1). Implants were washed in an ultrasonic cleaner with acetone and distilled water for 1 h, respectively, and dried in a 37 °C oven (control group; Figure 1a). For the alkali treatment, after washing with acetone and distilled water, samples were soaked in 20 ml per sample each of 5 N NaOH solution (NACALAI TESQUE, Inc., Kyoto, Japan) at 60 °C for 24 h with gentle shaking. The implants were then washed with distilled water and dried in 37 °C oven overnight (alkali group; Figure 1b).
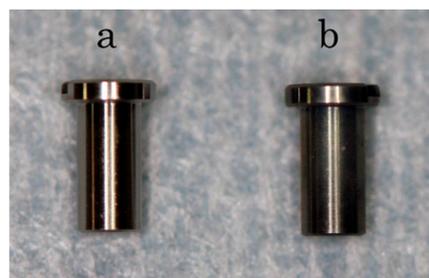

Figure 1. Pure titanium implants. Implant body: diameter, 2 mm; length, 4 mm. Implant head: diameter, 3 mm; height, 0.5 mm. (**a**) control implant (**b**) alkali hydrothermally-treated implant.

2.2. Analysis of Surface Structure

Each group of implants was placed on the sample stage with carbonate adhesive tape, then the implant surface was imaged by scanning electron microscopy (SEM; JSM-6010PLUS/LA, Nihon Denshi Oyo Co., Ltd., Tokyo, Japan) at ×3000 and ×40,000 magnification.

2.3. Wettability Test

Each implant was placed on the sample stage, and a 1 μL drop of pure water was gently applied to the bottom of the implant. Ten seconds after the droplet and implant touched, an image was taken with an S-image device (Excimer Inc., Kanagawa, Japan). The contact angles of the water drop were measured using the ImageJ program (National Institutes of Health, Bethesda, MD, USA). The contact angle values were obtained by the half-angle method; the angle of the end point and the vertex point of the droplet was measured, then doubled, and this value was the contact angle (n = 5).

2.4. Animal Experiment

The animal study was approved by the Research Facilities Committee for Laboratory Animal Science, Hiroshima University School of Medicine (Approved number A16-3). Five female New Zealand white rabbits (22 weeks old, 3.0–3.5 kg body weight) were used in this study. All procedures were performed under general anesthesia with sodium pentobarbital (10 mg/kg intravenously; Somnopentyl®, Kyoritsu Seiyaku Corporation, Tokyo, Japan) and local infiltration anesthesia with 2% lidocaine and 1:80.000 noradrenaline (Xylocaine®, Dentsply, Tokyo, Japan). Two implant sockets (diameter: 2 mm; depth: 4 mm) were created in both femurs with low-speed drilling using a ϕ2.0 mm round drill and a ϕ2.0 mm twist drill while injecting sufficient water. Then, the control group implants were placed in the left femur and the alkali group implants were placed in the right femur (Figure 2). Three weeks after the surgery, the animals were sacrificed, and bone tissue blocks containing the implants were obtained. All tissue blocks were immediately fixed in 10% neutral formalin.

Figure 2. Implant placement. Implants were inserted into pre-drilled bone sockets in the right and left femurs (two in each femur).

2.5. Removal Torque

After tissue fixation, the removal torque (RT) of each implant at the mesial side was recorded using a digital torque gauge (BTG-E100CN; Tonichi, Tokyo, Japan) (n = 5). The maximum torque to remove was measured as the RT value.

2.6. Histological Examination

The blocks with implants at the distal side were dehydrated using ascending concentrations of ethanol, cleared with acetone, and embedded in light-polymerized polyester resin (Technovit 7200VLC, Heraeus Kulzer, Wehrheim, Germany). Photo-polymerization equipment was used (BS5000, EXAKT Apparatebau, Norderstedt, Germany) to ensure complete polymerization and the specimens were sectioned with a high-precision diamond disc to produce 200-μm–thick cross-sections. Undecalcified specimens were ground to approximately 70-μm thickness with a grinding machine (MG5000, EXAKT

Apparatebau, Chemnitz, Germany) and stained with toluidine blue. A light microscope was used for histological examination of the specimens at ×3000 and ×40000 magnification.

2.7. Histomorphometric Examination

Using ImageJ, the obtained tissue specimen was examined for the bone–implant contact ratio (BIC), calculated as the length of the bone contact portion from the entire length of the implant body. The bone tissue area ratio (BTA) was calculated in sections of interest (0.5 mm width from both sides of the implant body) (Figure 3; combined yellow and black dotted areas). The BIC and BTA were measured separately for the cortical bone segment (upper yellow dot area) and the bone marrow segment (lower black dot area) of the femur (n = 5).
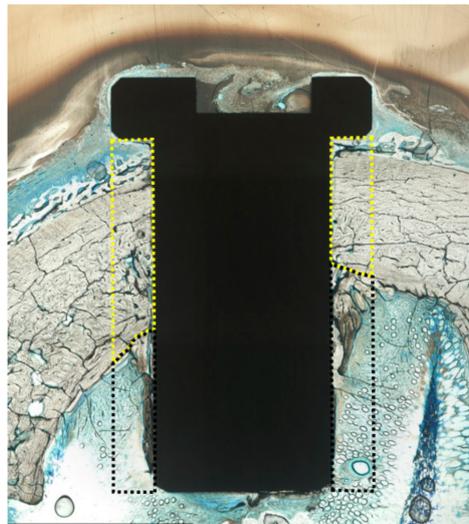

Figure 3. Histomorphometric analysis. The yellow and black dotted lines indicate the total area of interest, 0.5 mm width from the implant surface. Yellow dotted area: the cortical bone portion. Black dotted area: the bone marrow portion (×4 magnification).

2.8. Statistical Analysis

All data were analyzed at the 5% significance level using Student's *t* test, and were expressed as the mean ± standard deviation.

3. Results

3.1. Comparison of Surface Morphologies

In the control group, a regular polished surface was observed at ×3000 magnification (Figure 4a); at ×40,000 magnification, similarly polished images were observed, and a smooth surface structure was seen (Figure 4b). In the alkali group, a rough surface structure was observed at ×3000 magnification (Figure 4c). At ×40,000 magnification, a nano-sized pore structure was observed (Figure 4d).
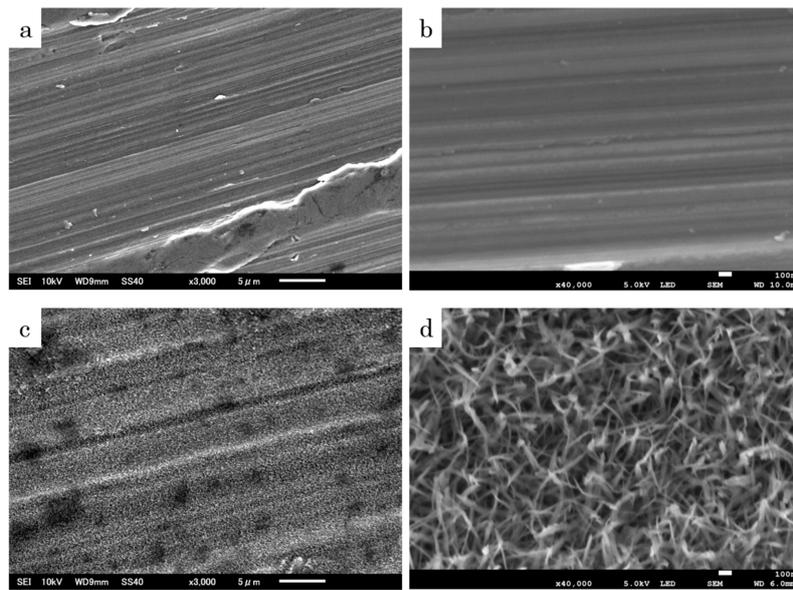
Figure 4. Scanning electron microscopy images. In the control group, a regular polished surface was observed at both ×3000 magnification (**a**) and ×40,000 magnification (**b**). In the alkali group, a rough surface structure was observed at ×3000 magnification (**c**), and a nanoscale pore structure was observed at ×40,000 magnification (**d**).

3.2. Wettability Test

In the control group, the shape of the water drop had a slightly expanded semicircular shape; the yellow line indicates the contact angle (Figure 5a). In contrast, in the alkali group, the droplet was spread widely and observation from the side was difficult (Figure 5b). Contact angles are reported in Table 1. In the alkali group, measurement was impossible because the contact angle was almost 0.

Table 1. Contact Angle.

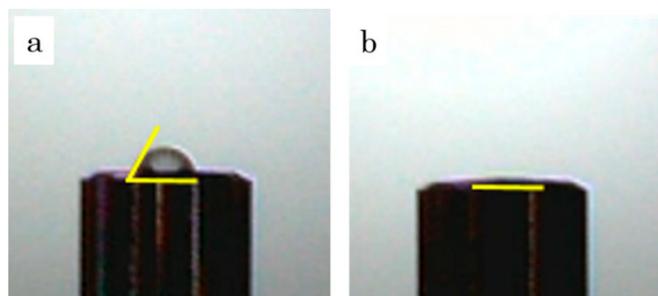| Group	°($\pm$SD)
Control	79.0 $\pm$ 2.3 *
Alkali	almost 0

SD: standard deviation; * $p < 0.01$.

Figure 5. Images of the wettability test. The yellow line indicates the contact angle of the dropped water. In the control group, a slightly expanded semicircular shape was observed (**a**). In the alkali group, the droplet was spread widely and observation from the side was difficult (**b**).

3.3. Removal Torque

The RT value was significantly higher in the alkali group than in the control group (Figure 6).
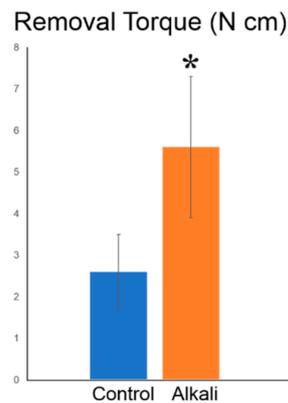

Figure 6. Removal torque (RT). The RT value was higher in the alkali group than in the control group. SD: standard deviation; * $p < 0.05$.

3.4. Histological and Histomorphometric Examination

A representative histological image from each group is shown in Figure 7. The BIC value and the BTA are reported in Figures 8 and 9, respectively. The bone width was almost idemtical in the cortical bone segments of both groups. The bone tissue formed toward the implant surface, and bone–implant contact was observed. The BTA of the cortical bone was not significantly different between the control and alkali groups. However, the BIC value was higher in the alkali group than in the control group. In the bone marrow segment, formed bone along the implant surface was observed in both groups. Bone formation was especially observed near the bottom of the implant in the alkali group. The BTA was higher in the alkali group than in the control group, and the BIC values were not significantly different. When examining the whole portion, there were significant differences in both BIC and BTA.
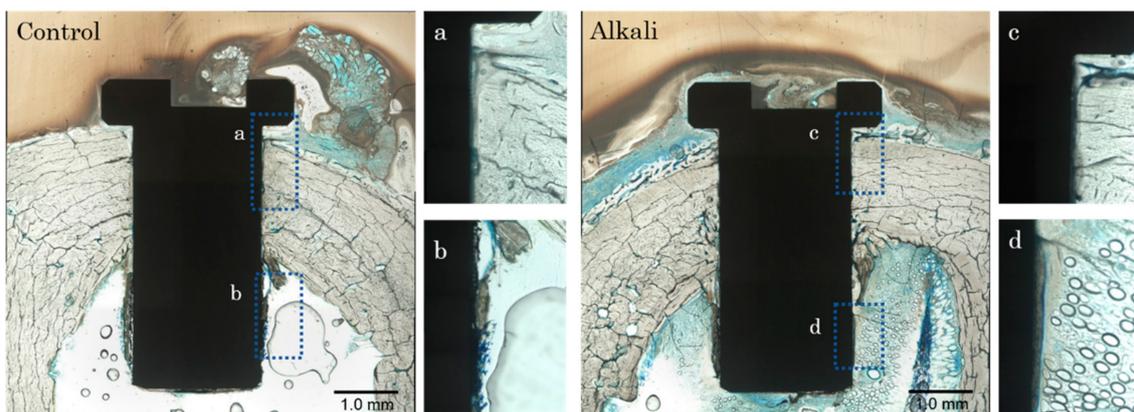

Figure 7. Histological images of the control and alkali groups. Control: ((**a**), cortical bone area) partial bone contact was observed at the bone/implant surface interface. Osseointegration was not detected upper portion. ((**b**), bone marrow area) a limited amount of bone tissue was observed on the surface. Alkali: ((**c**), cortical bone area) bone contact was observed and osseointegration detected around the surface. ((**d**), bone marrow area) bone formation was observed near the bottom. Bone formation occurred from the cortical bone portion.
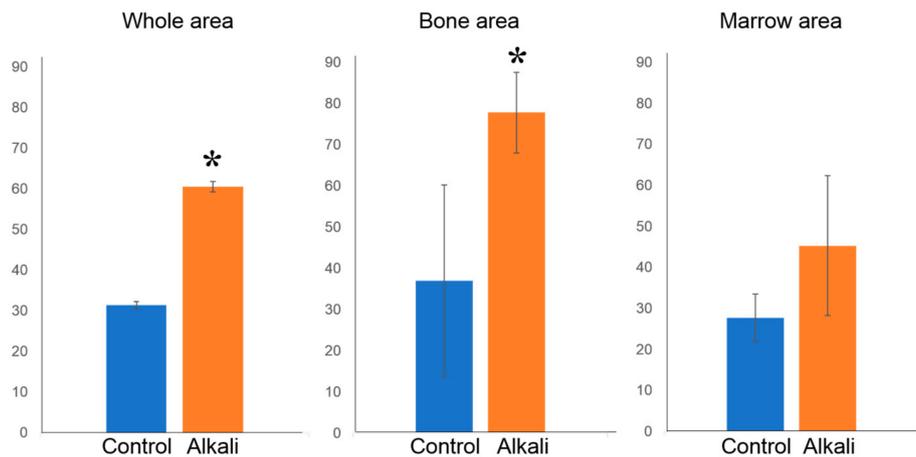
Figure 8. Bone implant contact ratio (%; BIC). The BIC values of the whole area and bone area were higher in the alkali group than in the control group. SD: standard deviation; * $p < 0.01$.
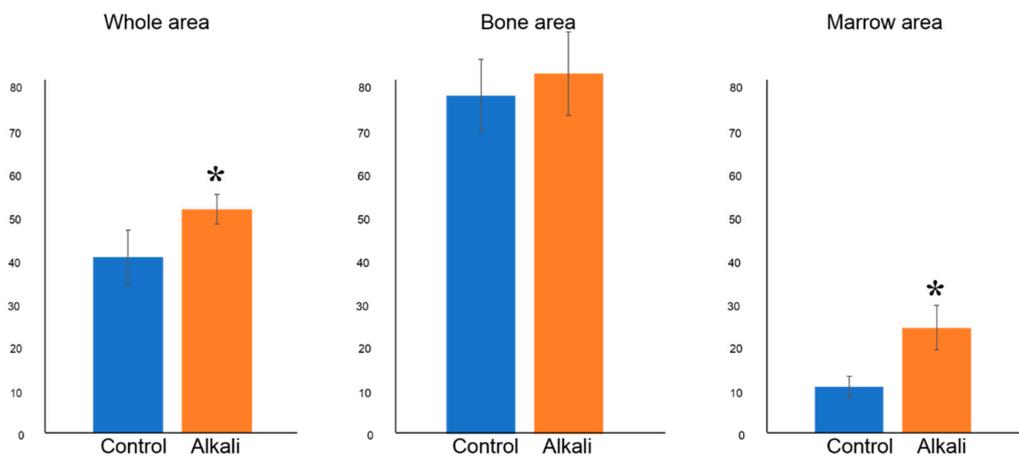

Figure 9. Bone tissue area ratio (%; BTA). The BTA values of the whole area and marrow area were higher in the alkali group than in the control group. SD: standard deviation; * $p < 0.01$.

4. Discussion

The results show that alkali hydrothermal treatment of titanium implants enhanced bone integration in the cortical portion and bone formation in the bone marrow portion of rabbit femurs *in vivo*.

Osseointegration is achieved by bone formation on the implant surface, which is largely associated with cell migration, cell adhesion, and cell differentiation [23].

Modification of the implant surface topography provides a suitable matrix for osteoblast cell adhesion, proliferation, differentiation, and bone formation. A modified titanium surface structure can potentially be applied in biomaterials. Alkali-treated titanium surfaces with nanostructures have been of great interest [22]. Alkali hydrothermal treatment of titanium can create a super hydrophilic titanate layer with nano-network structures. In the present study, the alkali hydrothermally-treated implant showed a modified surface with uniform nanostructure pores on SEM observation. Furthermore, examination of the contact angle during the wettability test indicated a super hydrophilic surface. These characteristics are consistent with those of previous reports [24,25]. There are other advantages of the alkali hydrothermal treatment method. Acid treatment and blasting processes produce a microscale roughened structure on the surface rather than the nanoscale surface produced by alkali hydrothermal treatment [6]. The blasting treatment may be difficult to process uniformly depending

on the composition of the target, such as those with a porous or fibrous structure. In acid treatment, there is concern that corrosion reduces the mechanical strength of metal objects.

However, alkali hydrothermal treatment is a simple chemical treatment, and any object can be treated uniformly. In addition, since this process forms a sodium titanate layer on the surface, there is little influence on the structure. To evaluate osseointegration, we performed histological observation and histomorphometric measurements. Measurements were performed in two areas and combined to a third one for analysis: the cortical bone portion, the bone marrow portion, and the whole portion comprising the area the length of the implant. Analysis of the whole portion was undertaken to evaluate implant stability in the surrounding bone. Analysis of the cortical bone portion evaluated the integration between bone and implant, because the implant was in contact with surrounding bone at placement. Finally, analysis of the bone marrow portion was undertaken to evaluate osseoinduction, because this portion was originally without bone.

Histological observations revealed osseointegration for both the alkali group and the control group. The BIC ratios in the whole portion and cortical bone portion were higher in the alkali group than in the control group. This result seems to be related to the higher bone integration at the cortical bone portion. Several studies have reported that the surface of alkali-treated titanium promotes osteoinduction by the nanoscale structure *in vitro*, the hydrophilicity of the surface promotes initial cell adhesion, and nutrient supply and is advantageous for bone regeneration at early stages [23,26]. Additionally, alkali-treated titanium forms an apatite layer on the surface in SBF [17–19]. When titanium is immersed in a NaOH solution and heated, an amorphous layer of alkali titanate is formed and strongly bonds to the substrate. When this alkali-treated titanium is soaked in SBF, alkali ions are eluted from the surface layer, the surface gel induces nucleation of apatite, and an apatite layer is formed [27]. This suggests that alkali-treated implants chemically integrate with the surrounding bone by apatite formation. Accordingly, alkali hydrothermally treated titanium implants are expected to induce excellent bone integration. In fact, several *in vivo* studies have reported on the benefits of alkali treatment of implant surfaces [28–30], and its strong effect on the chemical integration of implants with host bone. For these reasons, compared with the control group, the BIC of the alkali-treated implant showed higher values in the whole portion and the cortical bone portion.

The BTA in the whole portion and bone marrow portion were higher in the alkali group than in the control group. This seems to be associated with the high bone formation in the bone marrow portion, and it was opposite to the BIC measurement results. Parent bone already exists in the cortical bone portion; therefore, there was no difference in the BTA. Analysis of the bone marrow, which is initially without bone tissue, is useful to evaluate implant-associated osteoconduction and osteogenesis-promoting effects. As mentioned above, the nanostructure topography and super hydrophilic properties of the alkali-treated implant are advantageous for osteogenesis. This surface topography was assumed to enhance the surface bioactivity on implants and subsequently accelerate the early bone-to-implant healing process.

The BIC ratio of the alkali group was that of higher than the control group; however, the difference was not significant in marrow portion. This indicates that new bone formation had occurred by the evaluation period; however, bone remodeling was not yet complete. Therefore, the standard deviation of the measured value covered a large range.

The RT values of the alkali group were higher than those of the control group. The RT reflects a quantitative assessment of osseointegration of the entire implant. RT is strongly influenced by cortical bone integration and is strongly correlated with the BIC ratio [31–33]. According to the BIC and The RT measurements, the alkali group obtained excellent implant stability by achieving favorable osseointegration in the cortical bone portion. In addition, the increased strength of bone–implant integration around nanostructured surfaces is considered due to the increased surface area and mechanical integration between the nanosurfaces and the bone [34].

Camargo et al. demonstrated the material properties and bone formation of alkali-treated implants. However, the implants have a threads structure and cause mechanical irritation to the surrounding

bone at implantation. Therefore, it is considered that unspecified factors are involved in the evaluation of surface treatment on bone formation *in vivo*. In this study, we used cylinder shape implants without threads structure, and clarified the osteoconduction and bone integration abilities of alkali-treated implants *in vivo*.

Based on the results of the present study, we suggest that an alkali hydrothermally-treated implant could achieve favorable stability when placed in contact with the parent bone.

Alkali hydrothermal treatment of titanium implants results in the following: expansion of the contact surface area through creation of a nanopore structure, chemical bonding through the formation of an apatite layer, and promotion of osteoblast activation on the surface. These factors promote new bone formation on the implant surface and strong chemical integration.

Furthermore, the results of the present study indicate that it might be possible to promote bone formation around the bone marrow, an area without parent bone tissue.

5. Conclusions

Alkali hydrothermal surface treatment of titanium implants enhances bone integration in areas where the implant is in contact with bone and may promote osteoinduction. Alkali hydrothermal treatment is useful for improving implant stability due to osseointegration.

Author Contributions: Conceived and designed experiments: Kazuya Doi, Hanako Umehara. Performed experiments: Kazuya Doi, Reiko Kobatake, and Hanako Umehara. Analyzed the data: Hanako Umehara, Yoshifumi Oki, and Yusuke Makihara. Contributed reagents/materials/analysis tools: Kazuya Doi, Reiko Kobatake, Hanako Umehara, and Takayasu Kubo. Wrote the paper: Kazuya Doi, Reiko Kobatake, and Kazuhiro Tsuga.

Conflicts of Interest: The authors declare no conflict of interest.

References

1. Brånemark, P.; Zarb, G.; Albrektsson, T. *Tissue-Integrated Prostheses*; Quintessence Publishing: Hanover Park, IL, USA, 1985; pp. 11–43.
2. Buser, D.; Sennerby, L.; De Bruyn, H. Modern implant dentistry based on osseointegration: 50 Years of progress, current trends and open questions. *Periodontol 2000* **2017**, *73*, 7–21. [CrossRef]
3. Chappuis, V.; Buser, R.; Brägger, U.; Bornstein, M.M.; Salvi, G.E.; Buser, D. Long-term outcomes of dental implants with a titanium plasma-sprayed surface: A 20-year prospective case series study in partially edentulous patients. *Clin. Implant Dent. Relat. Res.* **2013**, *15*, 780–790. [CrossRef] [PubMed]
4. Niinomi, M. Recent research and development in titanium alloys for biomedical applications and healthcare goods. *Sci. Technol. Adv. Mater.* **2003**, *4*, 445–454. [CrossRef]
5. Le Guéhennec, L.; Soueidan, A.; Layrolle, P.; Amouriq, Y. Surface treatments of titanium dental implants for rapid osseointegration. *Dent. Mater.* **2007**, *23*, 844–854. [CrossRef] [PubMed]
6. Iwaya, Y.; Machigashira, M.; Kanbara, K.; Miyamoto, M.; Noguchi, K.; Izumi, Y.; Ban, S. Surface properties and biocompatibility of acid-etched titanium. *Dent. Mater. J.* **2008**, *27*, 415–421. [CrossRef] [PubMed]
7. Hamouda, I.M.; Enan, E.T.; Al-Wakeel, E.E.; Yousef, M.K. Alkali and heat treatment of titanium implant material for bioactivity. *Int. J. Oral Maxillofac. Implants* **2012**, *27*, 776–784. [PubMed]
8. Shi, X.; Nakagawa, M.; Kawachi, G.; Xu, L.; Ishikawa, K. Surface modification of titanium by hydrothermal treatment in Mg-containing solution and early osteoblast responses. *J. Mater. Sci. Mater. Med.* **2012**, *23*, 1281–1290. [CrossRef] [PubMed]
9. Jemat, A.; Ghazali, M.J.; Razali, M.; Otsuka, Y. Surface Modifications and their effects on titanium dental implants. *BioMed Res. Int.* **2015**, 791725. [CrossRef] [PubMed]
10. Offermanns, V.; Andersen, O.Z.; Riede, G.; Sillassen, M.; Jeppesen, C.S.; Almtoft, K.P.; Talasz, H.; Öhman-Mägi, C.; Lethaus, B.; Tolba, R.; et al. Effect of strontium surface-functionalized implants on early and late osseointegration: A histological, spectrometric and tomographic evaluation. *Acta Biomater.* **2018**, *15*, 385–394. [CrossRef] [PubMed]

11. Schwartz, Z.; Lohmann, C.H.; Oefinger, J.; Bonewald, L.F.; Dean, D.D.; Boyan, B.D. Implant surface characteristics modulate differentiation behavior of cells in the osteobl astic lineage. *Adv. Dent. Res.* **1999**, *13*, 38–48. [CrossRef] [PubMed]

12. Albrektsson, T.; Wennerberg, A. Oral implant surfaces: Part 1—Review focusing on topographic and chemical properties of different surfaces and in vivo responses to them. *Int. J. Prosthodont.* **2004**, *17*, 536–543.

13. Oliveira, P.T.; Zalzal, S.F.; Beloti, M.M.; Rosa, A.L.; Nanci, A. Enhancement of in vitro osteogenesis on titanium by chemically produced nanotopography. *J. Biomed. Mater. Res. A.* **2007**, *80*, 554–564. [CrossRef]

14. Yao, C.; Slamovich, E.B.; Webster, T.J. Enhanced osteoblast functions on anodized titanium with nanotube-like structures. *J. Biomed. Mater. Res. A.* **2008**, *85*, 157–166. [CrossRef] [PubMed]

15. Goldman, M.; Juodzbalys, G.; Vilkinis, V. Titanium surfaces with nanostructures influence on osteoblasts proliferation: A systematic review. *J. Oral Maxillofac. Res.* **2014**, *5*, e1. [CrossRef]

16. Karazisis, D.; Petronis, S.; Agheli, H.; Emanuelsson, L.; Norlindh, B.; Johansson, A.; Rasmusson, L.; Thomsen, P.; Omar, O. The influence of controlled surface nanotopography on the early biological events of osseointegration. *Acta Biomater.* **2017**, *15*, 559–571. [CrossRef] [PubMed]

17. Kokubo, T.; Miyaji, F.; Kim, H.M. Spontaneous formation of bone like apatite layer on chemically treated titanium metals. *J. Am. Ceram. Soc.* **1996**, *79*, 1127–1129. [CrossRef]

18. Ban, S.; Iwaya, Y.; Kono, H.; Sato, H. Surface modification of titanium by etching in concentrated sulfuric acid. *Dent. Mater.* **2006**, *22*, 1115–1120. [CrossRef] [PubMed]

19. Kono, H.; Miyamoto, M.; Ban, S. Bioactive Apatite coating on titanium using an alternate soaking process. *Dent. Mater. J.* **2007**, *26*, 186–193. [CrossRef] [PubMed]

20. Kobatake, R.; Doi, K.; Oki, Y.; Umehara, H.; Kawano, H.; Kubo, T.; Tsuga, K. Investigation of effective modification treatments for titanium membranes. *Appl. Sci.* **2017**, *7*, 1022. [CrossRef]

21. Zhuang, X.M.; Zhou, B.; Ouyang, J.L.; Sun, H.P.; Wu, Y.L.; Liu, Q.; Deng, F.L. Enhanced MC3T3-E1 preosteoblast response and bone formation on the addition of nano-needle and nano-porous features to microtopographical titanium surfaces. *Biomed. Mater.* **2014**, *9*, 045001. [CrossRef] [PubMed]

22. Xie, Y.; Yang, F.; Zheng, X.; Ding, C.; Dai, K.; Huang, L. Nano-structured titanium coating for improving biological performance. *Nanosci. Nanotechnol.* **2011**, *11*, 10770–10773. [CrossRef]

23. Mendonça, G.; Mendonça, D.B.; Aragão, F.J.; Cooper, L.F. Advancing dental implant surface technology—From micron- to nanotopography. *Biomaterials* **2008**, *29*, 3822–3835. [CrossRef] [PubMed]

24. Camargo, W.A.; Takemoto, S.; Hoekstra, J.W.; Leeuwenburgh, S.C.G.; Jansen, J.A.; van den Beucken, J.J.J.P.; Alghamdi, H.S. Effect of surface alkali-based treatment of titanium implants on ability to promote in vitro mineralization and in vivo bone formation. *Acta Biomater.* **2017**, *57*, 511–523. [CrossRef] [PubMed]

25. Kawai, T.; Takemoto, M.; Fujibayashi, S.; Akiyama, H.; Tanaka, M.; Yamaguchi, S.; Deepak, K.P.; Kenji, D.; Tomiharu, M.; Takashi, N.; et al. Osteoinduction on acid and heat treated porous Ti metal samples in canine muscle. *PLoS ONE* **2014**, *9*, e88366. [CrossRef] [PubMed]

26. Dalby, M.J.; McCloy, D.; Robertson, M.; Wilkinson, C.D.; Oreffo, R.O. Osteoprogenitor response to defined topographies with nanoscale depths. *Biomaterials* **2006**, *27*, 1306–1315. [CrossRef]

27. Kim, H.M.; Miyaji, F.; Kokubo, T.; Nakamura, T. Preparation of bioactive Ti and its alloys via simple chemical surface treatment. *J. Biomed. Mater. Res.* **1996**, *32*, 409–417. [CrossRef]

28. Nishiguchi, S.; Kato, H.; Neo, M.; Oka, M.; Kim, H.M.; Kokubo, T.; Nakamura, T. Alkali-and heat-treated porous titanium for orthopedic implants. *J. Biomed. Mater. Res.* **2001**, *54*, 198–208. [CrossRef]

29. Nishiguchi, S.; Fujibayashi, S.; Kim, H.M.; Kokubo, T.; Nakamura, T. Biology of alkali-and heat-treated titanium implants. *J. Biomed. Mater.* **2003**, *67*, 26–35. [CrossRef] [PubMed]

30. Chang, C.S.; Lee, T.M.; Chang, C.H.; Liu, J.K. The effect of microrough surface treatment on miniscrews used as orthodontic anchors. *Clin. Oral Implants Res.* **2009**, *20*, 1178–1184. [CrossRef] [PubMed]

31. Carlsson, L.; Röstlund, T.; Albrektsson, B.; Albrektsson, T. Removal torques for polished and rough titanium implants. *Int. J. Oral Maxillofac. Implants* **1988**, *3*, 21–24. [PubMed]

32. Oki, Y.; Doi, K.; Makihara, Y.; Kobatake, R.; Kubo, T.; Tsuga, K. Effects of continual intermittent administration of parathyroid hormone on implant stability in the presence of osteoporosis: An in vivo study using resonance frequency analysis in a rabbit model. *J. Appl. Oral Sci.* **2017**, *25*, 498–505. [CrossRef] [PubMed]

33. Okazaki, Y.; Doi, K.; Oki, Y.; Kobatake, R.; Abe, Y.; Tsuga, K. Enhanced osseointegration of a modified titanium implant with bound phospho-threonine: A preliminary in vivo study. *J. Funct. Biomater.* **2017**, *8*. [CrossRef] [PubMed]

34. Nishimura, I.; Huang, Y.; Butz, F.; Ogawa, T.; Lin, A.; Wang, C.J. Discrete deposition of hydroxyapatite nanoparticles on a titanium implant with predisposing substrate microtopography accelerated osseointegration. *Nanotechnology* **2007**, *18*, 245101. [CrossRef]